DOE/JPL/954862-1

DEVELOPMENT OF A MODEL AND COMPUTER CODE TO DESCRIBE SOLAR GRADE SILICON PRODUCTION PROCESSES

First Quarterly Report

By
R. K. Gould

February 1978

Work Performed Under Contract No. NAS-7-100-954862

AeroChem Research Laboratories, Incorporated
Princeton, New Jersey

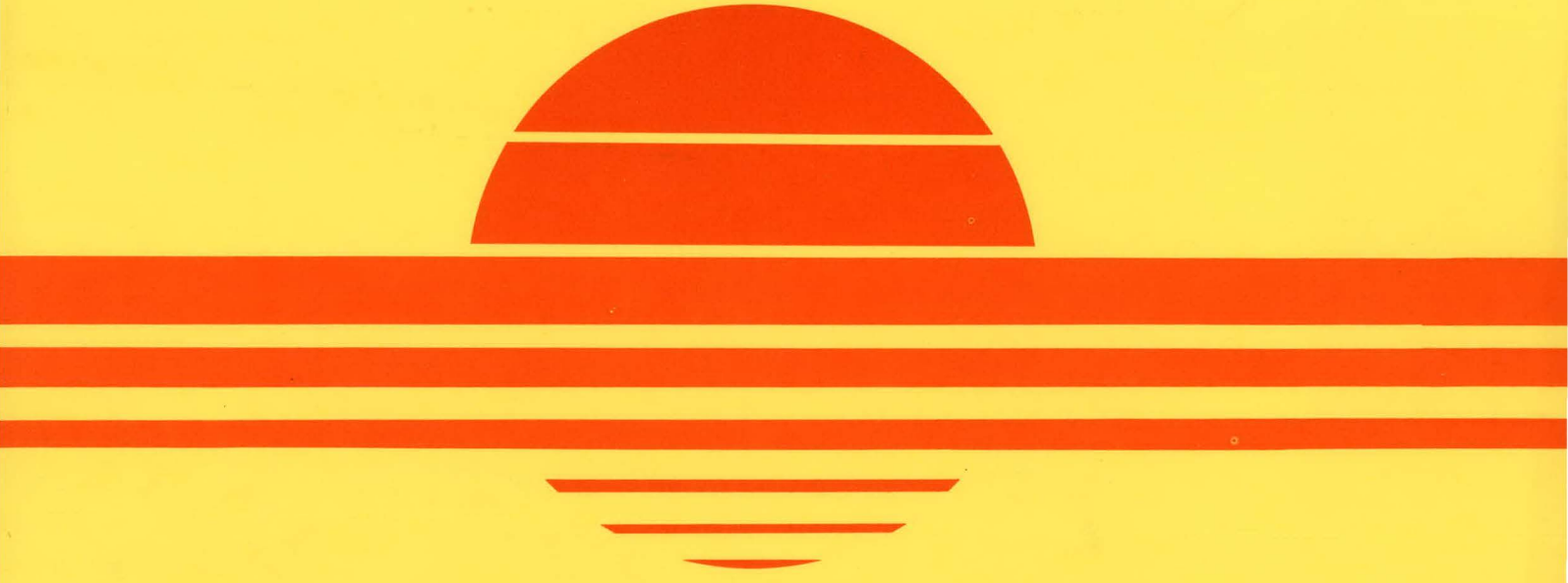

U.S. Department of Energy

Solar Energy

DISCLAIMER

NOTICE

AeroChem-TN-184

DOE/JPL/954862-1
Distribution Category UC-63b

DEVELOPMENT OF A MODEL AND COMPUTER CODE TO DESCRIBE SOLAR GRADE SILICON PRODUCTION PROCESSES

FIRST QUARTERLY REPORT

R. K. GOULD

FEBRUARY 1978

JPL Contract No. 954862
DRL Item No. 4, DRD No. QR
LSSA Silicon Material Task

Approved by

Hartwell F. Calcote
Director of Research

AeroChem Research Laboratories, Inc.
Princeton, New Jersey

FOREWORD AND ACKNOWLEDGMENTS

This is the first quarterly progress report covering the period 21 September 1977 to 31 December 1977. During this period the following people made significant contributions to the program: R.D. Thorpe and A. Bazelow.

ABSTRACT

This program aims at developing a mathematical model and a computer code based on this model, which will allow prediction of the product distribution in chemical reactors in which gaseous silicon compounds are converted to condensed-phase silicon. The reactors to be modeled are flow reactors in which silane or one of the halogenated silanes is thermally decomposed or reacted with an alkali metal, H_2 or H atoms. Because the product of interest is particulate silicon, processes which must be modeled, in addition to mixing and reaction of gas-phase reactants, include the nucleation and growth of condensed Si via coagulation, condensation, and heterogeneous reaction.

During this report period the most recent version of a free shear layer turbulent mixing code (LAPP) which treats finite rate, gas-phase chemistry has been acquired and documented to ascertain exactly the numerous changes the code has undergone in recent years. Equations describing particle dynamics have been formulated and are being coded. A code for calculating particle coagulation rates is available; it will be recoded, combined with a nucleation model, and inserted into the LAPP code. A model for calculating nucleation rates has been selected from among several alternatives; the rate coefficients and thermochemical information needed for its utilization are currently being developed.

TABLE OF CONTENTS

I. INTRODUCTION

This program aims at developing a mathematical model and a computer code based on this model, which will allow prediction of the product distribution, as a function of time, in chemical reactors in which gaseous silicon compounds are converted to condensed-phase silicon. The reactors to be modeled are flow reactors in which silane or one of the halogenated silanes is thermally decomposed or reacted with an alkali metal, H_2 or H atoms. Because the product of major interest is condensed-phase silicon, the model must allow calculation of its rate of formation (via chemical reaction followed by nucleation), and the growth rate of the particulate Si via coagulation, condensation, and heterogeneous reaction. Since the efficiency of the particulate Si collection process will depend on the particle size distribution of the Si this must also be computed.

The basic model and computer code to be used as a starting point in developing this model is a two dimensional, nonequilibrium, parallel stream mixing code which has been used for a number of years to treat systems in which parallel laminar or turbulent flows mix and undergo chemical reactions. This code, the Low Altitude Plume Program[1] (the LAPP code), treats only gas-phase chemistry; one of the major tasks will therefore be the inclusion of "particle chemistry", i.e., nucleation and particle growth. The code, as implied by its name, treats the fluid dynamics of an open system. Thus modifications will also be required to account for the presence of reactor side walls. This change will be effected by manipulation of boundary conditions. Finally, the reactor being modeled may allow for significant amounts of recirculation. This is particularly important if particulate products are returned upstream to provide nucleation sites. The rigorous inclusion of this effect would enormously complicate the code; the equations to be solved would become elliptic rather than parabolic, specification of downstream boundary conditions would be required, and the marching technique used in LAPP to solve the conservation equations would have to be abandoned. It is not likely that such a scheme, with the complicated chemistry needed to describe the situation,

could be solved. Therefore, here also, boundary conditions will be manipulated to test the effects of injecting reaction products into upstream sections of the code.*

During this quarter a recent version of LAPP has been acquired and fully flow-charted to document the numerous small changes made in the code as it has evolved over the last few years. Equations to describe the flow of particles in the gas and couple the momentum and energy interactions between the particles and gas have been formulated and are being coded in a form appropriate for LAPP. A model treating particle coagulation has been obtained from yet another code[2] (CRAM) and awaits recoding for insertion. A nucleation model[3] has tentatively been selected. The model treats nucleation from a gas-phase chemical kinetics point of view and is particularly suitable for use in LAPP. It avoids use of liquid droplet concepts (particularly the specification of a surface tension) and instead depends on the specification of rate coefficients and thermochemistry of molecular n-mers up to and including a critical size. Above this size, which is a function of the supersaturation ratio, n-mers may be considered particles with bulk condensed-phase properties.

II. TECHNICAL DISCUSSION

A. THE LAPP CODE

The LAPP code[1] treats axisymmetric systems in which flowing gases mix and react. The gas composition, velocity, and temperature are specified as arbitrary functions of r (the transverse coordinate) at x = 0 (the starting position for the flow, x being the longitudinal coordinate). Finite rate chemistry is computed within the context of mass, species, momentum, and energy conservation equations written in parabolic form. The species conservation equations, in which the chemical reaction rate equations appear, are solved using an implicit difference scheme which circumvents the extreme "stiffness"

---

* The procedure envisioned involves, for given geometries and mass flows, the estimation of the amount of recirculated gas entering the main flow along its length, making initial guesses as to its composition and iterating the code calculation with the composition of the recirculated gas updated after each iteration.

these equations exhibit near chemical equilibrium. The other equations are solved using a standard explicit difference integration scheme.

1. Conservation Equations and Boundary Conditions

The following equations describe the free-shear layer turbulent or laminar mixing of co-flowing axisymmetric streams undergoing chemical reactions. For turbulent flow all properties are interpreted to be the mean (time-averaged) values. The eddy viscosity, μ, is then described by one of the phenomenological expressions given in Section II.A.5 (nomenclature is given in Table I).

Global Continuity

$$\frac{\partial}{\partial x}(\rho u) + \frac{1}{r}\frac{\partial}{\partial r}(\rho v r) = 0 \tag{1}$$

Conservation of Species

$$\rho u \frac{\partial F_i}{\partial x} + \rho v \frac{\partial F_i}{\partial r} = \frac{1}{r}\frac{\partial}{\partial r}\left(\frac{Le}{Pr}\,\mu r \frac{\partial F_i}{\partial r}\right) + \dot{w}_i \tag{2}$$

Conservation of Momentum

$$\rho u \frac{\partial u}{\partial x} + \rho v \frac{\partial u}{\partial r} = -\frac{dp}{dx} + \frac{1}{r}\frac{\partial}{\partial r}\left(\mu r \frac{\partial u}{\partial r}\right) \tag{3}$$

Conservation of Energy

$$\rho c_p \left[u \frac{\partial T}{\partial x} + v \frac{\partial T}{\partial r}\right] = u \frac{dp}{dx} + \mu\left(\frac{\partial u}{\partial r}\right)^2 + \frac{1}{r}\frac{\partial}{\partial r}\left[\frac{c_p}{Pr}\,\mu r \frac{\partial T}{\partial r}\right] + \mu \frac{Le}{Pr}\frac{\partial T}{\partial r}\sum_i c_{p_i}\frac{\partial F_i}{\partial r} - \sum_i \dot{w}_i h_i \tag{4}$$

State

$$\rho = \frac{pW}{RT} \tag{5}$$

The conservation equations are solved subject to the following initial and boundary conditions:

$$x = 0: \quad u = u(r), \quad F_i = F_i(r), \quad T = T(r)$$

$$r = 0: \quad \frac{\partial u}{\partial r} = \frac{\partial T}{\partial r} = \frac{\partial F_i}{\partial r} = 0$$

$$r \to \infty: \quad u \to u_e, \; F_i \to (F_i)_e, \; T \to T_e \tag{6}$$

Pressure is allowed to vary in the axial direction according to,

$$p = c_o + c_1 x + c_2 x^2 + c_3 x^3 \tag{7}$$

where c_o, c_1, c_2, and c_3 are input coefficients.

2. Transformation to Stream Function Coordinates

It is convenient to transform the equations into a streamline coordinate system and utilize the stream function, Ψ, as the radial coordinate. The transformation from cartesian (x, r) coordinates to streamline (x, Ψ) coordinates (which automatically satisfies global continuity, Eq. (1)) is defined by:

$$\Psi \frac{\partial \Psi}{\partial r} = \rho u r \tag{8a}$$

$$\Psi \frac{\partial \Psi}{\partial x} = -\rho v r \tag{8b}$$

From Eqs. (8a) and (8b) we obtain,

$$\left(\frac{\partial}{\partial r}\right)_x = \frac{\rho u r}{\Psi} \left(\frac{\partial}{\partial \Psi}\right)_x \tag{9a}$$

$$\left(\frac{\partial}{\partial x}\right)_r = \left(\frac{\partial}{\partial x}\right)_\Psi - \frac{\rho v r}{\Psi} \left(\frac{\partial}{\partial \Psi}\right)_x \tag{9b}$$

Introducing Eqs. (9a) and (9b) into Eqs. (2), (3), and (4), gives:

Species

$$\frac{\partial F_i}{\partial x} = \frac{1}{\Psi} \frac{\partial}{\partial \Psi}\left[\left(\frac{Le}{Pr}\right) \frac{\mu \rho u r^2}{\Psi} \frac{\partial F_i}{\partial \Psi}\right] + \frac{\dot{w}_i}{u\rho} \tag{10a}$$

and, on the axis of symmetry, $r = \Psi = 0$

$$\frac{\partial F_i}{\partial x} = 2\mu \left(\frac{Le}{Pr}\right) \frac{\partial^2 F_i}{\partial \Psi^2} + \frac{\dot{w}_i}{u\rho} \tag{10b}$$

Momentum

$$\frac{\partial u}{\partial x} = -\frac{1}{\rho u}\frac{dp}{dx} + \frac{1}{\Psi}\frac{\partial}{\partial \Psi}\left[\frac{\mu \rho u r^2}{\Psi}\frac{\partial u}{\partial \Psi}\right] \tag{11a}$$

and, on the axis of symmetry, $r = \Psi = 0$

$$\frac{\partial u}{\partial x} = -\frac{1}{\rho u}\frac{dp}{dx} + 2\mu\frac{\partial^2 u}{\partial \Psi^2} \tag{11b}$$

Energy

$$c_p\frac{\partial T}{\partial x} = \frac{1}{\rho}\frac{dp}{dx} - \frac{1}{\rho u}\sum_i h_i \dot{w}_i + \frac{1}{\Psi}\frac{\partial}{\partial \Psi}\left[\frac{c_p}{Pr}\frac{\mu \rho u r^2}{\Psi}\frac{\partial T}{\partial \Psi}\right] + \frac{\mu \rho u r^2}{\Psi^2}\left[\left(\frac{\partial u}{\partial \Psi}\right)^2 + \frac{Le}{Pr}\frac{\partial T}{\partial \Psi}\sum_i c_{p_i}\frac{\partial F_i}{\partial \Psi}\right] \tag{12a}$$

and, on the axis of symmetry, $r = \Psi = 0$

$$c_p\frac{\partial T}{\partial x} = \frac{1}{\rho}\frac{dp}{dx} + 2\mu\left(\frac{c_p}{Pr}\right)\frac{\partial^2 T}{\partial \Psi^2} - \frac{1}{\rho u}\sum_i h_i \dot{w}_i \tag{12b}$$

The governing set of parabolic partial differential equations, (Eqs. (10), (11) and (12)), are rewritten in finite difference form and then solved using a forward marching technique. The chemistry terms, $\dot{w}_i$, in the species continuity equations are evaluated via implicit differences; the diffusion terms in the species continuity equations and the complete energy and momentum equations are evaluated via explicit differences. The finite difference equations actually solved are given in Ref. 1; the techniques involved are given in Ref. 4.

3. Chemical Reaction Rate Equations

Ten possible reaction types are currently included in the program:

Reaction Type

(1) $A + B \rightleftarrows C + D$

(2) $A + B + M \rightleftarrows C + M$

(3) $A + B \rightleftarrows C + D + E$

(4) $A + B \rightleftharpoons C$

(5) $A + M \rightleftharpoons C + D + M$

(6) $A + B \rightarrow C + D$

(7) $A + B + M \rightarrow C + M$

(8) $A + B \rightarrow C + D + E$

(9) $A + B \rightarrow C$

(10) $A + M \rightarrow C + D + M$

Reaction types (6)-(10) correspond to reaction types (1)-(5), but proceed in the forward direction only. In Reactions (2), (5), (7), and (10), M is an arbitrary third body. In this program, all species are assumed to have equal third-body efficiencies; thus, in evaluating $\dot{w}^{(j)}$, $F_M = (W)^{-1}$. The net rates of production for all reactions are written below, in the form, $\dot{w}^{(j)} = RP^{(j)} - RM^{(j)}$.*

(1) $$\dot{w}^{(j)} = k_f \rho^2 F_A F_B - \frac{k_f \rho^2 F_C F_D}{K_p}$$

(2) $$\dot{w}^{(j)} = \frac{k_f \rho^3 F_A F_B}{W} - \frac{k_f \rho^2 F_C}{K_p WRT}$$

(3) $$\dot{w}^{(j)} = k_f \rho^2 F_A F_B - \frac{k_f \rho^3 F_C F_D F_E RT}{K_p}$$

(4) $$\dot{w}^{(j)} = k_f \rho^2 F_A F_B - \frac{k_f \rho^3 F_C}{K_p RT}$$

(5) $$\dot{w}^{(j)} = \frac{k_f \rho^2 F_A}{W} - \frac{k_f \rho^3 F_C F_D RT}{K_p W}$$

(6) $$\dot{w}^{(j)} = k_f \rho^2 F_A F_B$$

(7) $$\dot{w}^{(j)} = \frac{k_f \rho^3 F_A F_B}{W}$$

---

* The symbols RP and RM are used on the computer output.

(8) $$\dot{w}^{(j)} = k_f \rho^2 F_A F_B$$

(9) $$\dot{w}^{(j)} = k_f \rho^2 F_A F_B$$

(10) $$\dot{w}^{(j)} = \frac{k_f \rho^2 F_A}{W}$$

To reduce round-off and truncation errors $RP^{(j)}$ and $RM^{(j)}$ are computed separately for each reaction. All contributions to the molar rate of production of a given species are then computed and added algebraically to form $\dot{w}_i$.

The forward rate coefficient, k_f, is expressed in the form

$$k_f = AT^{-N} \exp(B/RT) \tag{13}$$

and K_p is determined from,

$$\ln K_p = -\Delta G/RT \tag{14}$$

The rate coefficients are currently divided into seven types:

Rate Coefficient Type

(1) $k_f = A$

(2) $k_f = AT^{-1}$

(3) $k_f = AT^{-2}$

(4) $k_f = AT^{-1/2}$

(5) $k_f = A \exp(B/RT)$

(6) $k_f = AT^{-1} \exp(B/RT)$

(7) $k_f = AT^{-3/2}$

4. Thermodynamic Data

The thermodynamic properties (specific heat, Gibbs free energy, and enthalpy) for each species are input to the program as c_{p_i}, $-\left(\frac{g_i - h_{298_i}}{T}\right)$ and $(h_i - h_{298})$ in tabular form as a function of temperature. Linear interpolation is used to define thermodynamic properties at the local temperature. Such data can, for many species, be found in the JANAF

Thermochemical Tables.[5] Where no such source exists, these quantities will be estimated in the best way available. (It should be kept in mind that any reasonable estimate is almost certainly better than exclusion of a species from the reaction scheme.)

5. Turbulent Eddy Viscosity Models

The following eddy viscosity models[6-9] are incorporated into the program:

Model 1 (Ferri)[6]

Initial region,*

$$\mu = \rho \varepsilon = \alpha 0.00137 \times |\rho_o u_o - \rho_e u_e| \tag{15a}$$

Developed region,

$$\mu = \rho \varepsilon = \alpha K \, b_{1/2} \, |\rho_o u_o - \rho_e u_e| \tag{15b}$$

where $b_{1/2}$ is the value of r where $\rho u = (\rho_o u_e + \rho_e u_e)/2$ and K is the eddy viscosity coefficient, usually taken to be 0.025.†

Model 2 (Ting/Libby)[8]

$$\mu = \rho \varepsilon = \alpha K \, \bar{r}_{1/2} |u_o - u_e| \, \rho \left(\frac{\rho_o}{\rho}\right)^2 \left(\frac{\eta}{r}\right)^2 \tag{16}$$

where

$$\eta^2 = 2 \int_o^r (\rho_o/\rho) \, r' \, d \, r' \tag{17}$$

and $\bar{r}_{1/2}$ is the value of η where $u = (u_o + u_e)/2$.

---

* Defined as region upstream of axial position where $(u_o - u_e)/(u_j - u_e) = 0.95$.

† Most of the models contain a numerical coefficient K which must be determined empirically. The value K = 0.025, taken from Schlicting,[7] has been incorporated directly into the program. This can be changed by the program input data via an appropriate value for the additional constant, α, Eqs. (15) - (21).

Model 3

Initial region,

$$\mu = \rho \varepsilon = \alpha 0.00137 \times \rho_o |u_o - u_e| \tag{18a}$$

Developed region,

$$\mu = \alpha K r_{1/2} \rho_o |u_o - u_e| \tag{18b}$$

where $r_{1/2}$ is the value of r where $u = (u_o - u_e)/2$.

Model 4

Initial region,

$$\mu = \rho \varepsilon = \alpha 0.00137 \times \rho_e |u_o - u_e| \tag{19a}$$

Developed region,

$$\mu = \rho \varepsilon = \alpha K r_{1/2} \rho \varepsilon |u_o - u_e| \tag{19b}$$

Model 5*(Ting/Libby)[8]

Initial region,

$$\mu = \rho \varepsilon = \alpha 0.00137 \times |u_j - u_e| \rho \left(\frac{\rho_j}{\rho}\right)^2 \tag{20}$$

Developed region,

$$\mu = \rho \varepsilon = \alpha K \bar{r}_{1/2} |u_o - u_e| \rho \left(\frac{\rho_o}{\rho}\right)^2 \left(\frac{\eta}{r}\right)^2 \tag{16}$$

Model 6 (Donaldson/Gray[9]

Initial region,

$$\mu = \rho \varepsilon = \alpha \bar{K} (r_{1/2} - r_{in}) \rho |u_o - u_e|/2 \tag{21a}$$

---

* In the program, the specification of Model 5 means that Eq. (20) will be used in the initial region and Model 2 (Eq. (16)) will be used in the developed region. This is important for re-starting a problem in the developed region for which Model 5 was selected to run from x = 0.

For $M_{1/2} \leq 1.2$ $\quad \bar{K} = 0.0468 + M_{1/2}\,[-0.0460\, M_{1/2} + 0.0256\, M_{1/2}^2]$

$M_{1/2} > 1.2$ $\quad \bar{K} = 0.0248$ (22)

where $M_{1/2}$ is the value of the Mach number where $u = (u_o + u_e)/2$ (i.e., the half radius). The speed of sound at the half radius, $a_{1/2}$ is expressed by,

$$a_{1/2} = \left[\frac{c_p}{c_p - (R/W_{1/2})} \frac{RT_{1/2}}{W_{1/2}} \right]^{1/2} \tag{23}$$

where $W_{1/2}$ and $T_{1/2}$ are evaluated at the half radius. In Eq. (21a), r_{in} is the inner mixing zone radius and is defined as the value of r where $(u_o - u_e)/(u_j - u_e) = 0.95$.

Developed region,

$$\mu = \rho\, \varepsilon = \alpha \bar{K}\, r_{1/2}\, \rho |u_o - u_e|/2 \tag{21b}$$

Laminar Flow

Sutherland's Law[10] is used to describe the viscosity as a function of temperature.

B. GAS/PARTICLE DYNAMICS

Small particles will (i) follow the gas streamline as they are carried along and (ii) adjust rapidly to the temperature of the surrounding gas (although phase changes such as fusion may result in sizeable transfers of energy to or from the gas). Thus little exchange of momentum or energy will occur (with the notable exception of phase change just mentioned). Large particles, on the other hand, will slip in the gas and may find themselves at a temperature significantly different from the surrounding gas. Thus, to treat flows in which heavy particle loadings result in large gas/particle interaction, it is necessary to modify the gas momentum and energy equations to include this interaction and to introduce the momentum and energy equations of these larger particles. The following terms (24) and (25) must thus be added to the momentum and energy equations, respectively, (Eqs. (3), (4), and (11), (12) to account for this momentum and energy exchange.

Momentum

$$-9/2u \sum_j \frac{F_{p_j} f_{p_j} \mu_g}{\rho_p r_j^2} \left(u - u_{p_j}\right) \tag{24}$$

Energy

$$9/2u \sum_j \frac{F_{p_j} f_{p_j} \mu_g}{\rho_p r_j^2} \left[\left(u - u_{p_j}\right)^2 + 2/3 \frac{C_p}{Pr} \frac{g_{p_j}}{f_{p_j}} \left(T_{p_j} - T\right)\right] \tag{25}$$

The indicated sums are over the particle mass classes.

The species equations for each particle mass class can be written in a form similar to Eqs. (2) and (10), i.e., in (x, r) coordinates

Particle Species

$$\rho u_{p_i} \frac{\partial F_{p_i}}{\partial x} + \rho v_{p_i} \frac{\partial F_{p_i}}{\partial r} = 1/r \frac{\partial}{\partial r}\left(\frac{Le}{Pr} \mu_{p_i} r \frac{\partial F_{p_i}}{\partial r}\right) + \dot{w}_{p_i} \tag{26}$$

or, in (x, Ψ) coordinates

$$\frac{\partial F_{p_i}}{\partial x} = \frac{1}{\Psi} \frac{\partial}{\partial \Psi}\left[\left(\frac{Le}{Pr}\right) \frac{\mu_{p_i} \rho u_{p_i} r^2}{\Psi} \frac{\partial F_{p_i}}{\partial \Psi}\right] + \frac{\dot{w}_i}{u_{p_i} \rho} \tag{27}$$

The equations describing the energy and momentum of the particles themselves are the following:

Particle Momentum

$$\frac{\partial u_{p_i}}{\partial x} = \frac{9}{2} \frac{f_{p_i} \mu_g}{\rho_p r_i^2} \left(u - u_{p_i}\right) \tag{28}$$

Particle Energy

$$u_{p_j} C_{p_p} \left(\frac{d T_{p_j}}{dx}\right) = - \frac{3 \mu_g g_{p_j}}{\rho_p r_j^2} \frac{C_p}{Pr} \left(T_{p_j} - T\right) - \frac{3\epsilon\sigma}{r_j \rho_p} \left(T_{p_j} - T_w\right)^4 \quad (29)$$

For small particles, it can be seen from Eqs. (24), (25), (28), and (29) that $u_{p_j} \rightarrow u$ and $T_{p_j} \rightarrow T$. A suitable criterion is now being sought to reduce the length of the calculation by excluding from Eqs. (28) and (29) those particle mass classes for which momentum and energy exchange with the gas is negligible. These small particle mass classes would then be treated in a manner identical to that for molecular species. Also to be determined are models for the estimation of particle diffusivities, μ_{p_1}, and heat transfer coefficients, g_{p_j}. These quantities will be functions of the turbulence properties of the flow. Physically, these problems result from the fact that particles of sufficient size will cease to follow fluctuation in the flow and will thus (i) diffuse less rapidly and (ii) transfer heat more rapidly than would very small particles (or molecules).

C. PARTICLE CHEMISTRY

1. Nucleation

In systems in which large supersaturation ratios occur, such as those of interest here, it is attractive to employ a nucleation model[3] in which a limited series of simple gas-phase addition reactions are written which result in a "critical nucleus" above which growth to particle species with bulk properties is rapid. Such a model recommends itself because (i) it fits naturally into the gas-phase chemical kinetics format of the LAPP code and (ii) it avoids the use of "liquid drop" models which utilize bulk surface tensions which, for small n-mers ($n \approx 10\text{-}10^2$ atoms), are difficult to justify. Such a model has recently been proposed and used to treat iron particle nucleation in shock-tube studies in which Fe(CO) was thermally decomposed.

The model is described in detail in Ref. 3. Briefly, for silicon nucleation, a series of reactions is assumed to occur†:

$$Si_n + Si \rightleftarrows Si^*_{n+1} \tag{30}$$

$$Si^*_{n+1} + M \rightarrow Si_{n+1} + M \tag{31}$$

The lifetimes of the transition complexes $(Si)_{n+1}$ increase with n and thus the kinetics change from three-body to two-body as n increases. A simple hard-sphere model is assumed to obtain a rate coefficient for the forward three-body overall reaction rate coefficient

$$Si_n + Si + M \underset{k_{r,n}}{\overset{k_{f,n}}{\rightleftarrows}} Si_{n+1} + M \tag{32}$$

and the backward reaction rate coefficient is obtained by estimating the standard condition free energies for the n-mers and using

$$\frac{k_{f,n}}{k_{r,n}} = k_B T \exp\left[-\frac{\Delta G^\circ(Si_{n+1}) - \Delta G^\circ(Si_n) - \Delta G^\circ(Si)}{RT}\right] \tag{33}$$

The use of this model leads to a definition of a "critical nucleus" for that $n = n^*$ at which $k_{f,n} = k_{f,n-1} = k_{r,n} = k_{r,n-1}$. At n^* a "bottleneck" is observed in the n-mer concentration. Above n^* n-mer growth is rapid and individual species concentrations are relatively decreasingly dependent on n. Below n^*, the n-mer concentration decreases rapidly with increasing molecular weight; growth is slow due to the bottleneck at n^*.

The application of this model provides a source for particles. Once n-mers pass through a size, say five atoms above the critical size, they will be considered as particulate matter which has the dynamic properties of the

---

† Only monomer addition need be considered since $F_{Si} >> F_{Si_2}$. Also, more complicated reactions such as, e.g., $Si_n + SiCl_{2x} \rightarrow Si_{n+1} + xCl_2$ will not be considered until this basic model is developed. Also the possibility of polymer formation $(SiCl_x)_n$ can be treated if analysis of products from experiments indicates that such species are prevalent.

bulk material. If $\dot{w}^s_{p_1}$ and $\dot{w}^s_{p_2}$ are rates of creation of particles with masses m_1 and m_2 by nucleation and $m_1 < m_{n^*} < m_2$, then the following equation describes particle formation

$$w_{Si_{n^*+5}} = R_{Si_{n^*+5,1}} \dot{w}^s_{p_1} + \left(1 - R_{Si_{n^*+5}}\right) \dot{w}^s_{p_2} \tag{34}$$

where $R_{Si_{n^*+5,1}}$ is a fraction given by

$$R_{Si_{n^*+5,1}} = \frac{m_2 - \left(m_1 + m_{Si_{n^*+5}}\right)}{m_2 - m_1} \tag{35}$$

which is chosen to conserve mass and particle number.

Work on determining the rate coefficients for n-mer growth and the thermodynamic properties of the n-mers using the model of Ref. 3 is proceeding. The next step will be the actual coding of this model and the coagulation model described below.

2. Coagulation

The coagulation model to be used is described fully in Refs. 2 and 11. The model assumes that particles coagulate as a result of random motion brought about by diffusion (both Brownian and turbulent) or by inertial effects in which the particles have non-zero, mass-dependent average velocities relative to the gas brought about by gravity, large scale rotational motion, or strong shearing of the gas. To formulate the model, particles are divided into mass classes $\{m_i\}_{i=1,r}$ where

$$m_i = \alpha^{i-1} m_1 \tag{36}$$

The factor α should be as small as possible for accuracy; because of calculation time considerations it will probably be set at 10 which results in a rather minor overestimation[2] of the rate of growth of the particles. The rate of formation of particles of mass m_i via coagulation is given by

$$\dot{w}^{C}_{p_i} = -\sum_{j=1}^{r} K_{ij}\,\rho^2\,F_{p_i}\,F_{p_j} + \sum_{j=1}^{i} S_{ij}\,K_{ij}\,R_{ij}\,\rho^2\,F_{p_i}\,F_{p_j} + \sum_{j=1}^{i-1} S_{i-1,j}\,K_{i-1,j}\,(1-R_{ij})\rho^2\,F_{p_i}\,F_{p_j} \tag{37}$$

The fraction R_{ij}, required to insure mass conservation, is given by

$$R_{ij} = \frac{m_{i+1} - (m_i + m_j)}{m_{i+1} - m_i} \tag{38}$$

S_{ij} is a factor which insures correct counting when particles of the same mass collide

$$S_{ij} = \begin{cases} 1/2 & 1 = j \\ 1 & i \neq j \end{cases} \tag{39}$$

The rate coefficients for coagulation, K_{ij}, are sums of coefficients representing the various operative mechanisms, i.e., Brownian diffusion, turbulence-enhanced coagulation, coagulation due to the sedimentation of heavy, large particles, and shear-enhanced coagulation.

$$K_{ij} = K^{Br}_{ij} + K^{turb}_{ij} + K^{g}_{ij} + K^{Sh}_{ij} \tag{40}$$

Brownian Coagulation[12]

$$K^{Br}_{ij} = 4\pi(r_i + r_j)(D_i + D_j)\left\{\frac{r_i + r_j}{r_i + r_j + \delta_{ij}} + \frac{4(D_i + D_j)}{(r_i + r_j)G_{ij}}\right\}^{-1} \tag{41}$$

where D_i is the particle diffusion coefficient

$$D_i = \frac{k_B T}{6\pi\,\mu_g\,r_i}\left[1 + 1.26\,\frac{\lambda_g}{r_i} + 0.4\,\frac{\lambda_g}{r_i}\,\exp\left(-\frac{1.1\,r_i}{\lambda_g}\right)\right] \tag{42}$$

G_{ij} is the mean relative particle velocity

$$G_{ij} = \left[\left(\frac{1}{m_i} + \frac{1}{m_j}\right)\frac{8k_B T}{\pi}\right]^{1/2} \tag{43}$$

δ_{ij} is a particle mean free path

$$\delta_{ij} = (\delta_i^2 + \delta_i^2)^{1/2} \tag{44}$$

$$\delta_i = \frac{2^{1/2}}{48} \frac{\pi G_i}{D_i r_i} \left[\left(2 r_i + \frac{8 D_i}{\pi G_i} \right)^3 - \left(4r_i^2 + \left(\frac{8 D_i}{\pi G_i} \right)^2 \right)^{3/2} \right] \tag{45}$$

The following simplified expression will be employed for certain cases:

For large particles with $Kn_i = \frac{\lambda g}{r_i} << 1$

$$K_{ij}^{Br} \approx \frac{2}{3} \frac{k_B T}{\mu_g} (r_i + r_j) \left(\frac{1}{r_i} + \frac{1}{r_j} \right) \tag{46}$$

If $Kn_i << 1$ and $Kn_j >> 1$

$$K_{ij}^{Br} \approx \pi r_i^2 G_j \tag{47}$$

For Kn_i and $Kn_j >> 1$

$$K_{ij}^{Br} \approx \pi (r_i + r_j)^2 G_{ij} \tag{48}$$

The >> sign in this case tentatively means $\gtrsim$ a factor of 10.

Turbulence-Enhanced Coagulation[13]

$$K_{ij}^{turb} = \pi \frac{\rho_p}{\rho} \frac{E_o^{3/4}}{\nu^{5/4}} (r_i + r_j^2) \left| (r_i^2 - r_j^2) \right| \tag{49}$$

where E_o, the turbulent energy dissipation rate per unit mass is given by

$$E_o = \frac{(\nu \, Re)^3}{\ell^4} \tag{50}$$

For consistency the length scale ℓ used in Eq. (50) is that used in the turbulent eddy viscosity model chosen (Section II.A.5).

Gravitational-Enhanced Coagulation[12]

$$K_{ij}^{g} = \xi_{ij} \pi (r_{max})^2 \left| v_{g,i} - v_{g,j} \right| \tag{51}$$

$$\delta_{ij} = \left(1 + \frac{r_{min}}{r_{max}}\right)^2 - \frac{1}{1 + \frac{r_{min}}{r_{max}}} \tag{52}$$

where

$$r_{min} = \begin{cases} r_i, & i < j \\ r_j, & i > j \end{cases} \tag{53}$$

$$r_{max} = \begin{cases} r_i & i \geqq j \\ r_j & i \geqq j \end{cases} \tag{54}$$

and

$$v_{g,i} = \frac{m_i \, g \, D_i}{k_B T} \qquad r_i \leqq 25 \ \mu m \tag{55}$$

and, for very large particles ($r_i > 25$ μm), $v_{g,i}$ must be found by solving Eq. (56)[12]

$$\frac{4 \, \mu_g^{1/3}}{(2 \, r_i \, \rho)^{1/3}} \, v_{g,i}^{5/3} + 12 \frac{\mu_g}{r_i \, \rho} \, v_{g,i} - \frac{8}{3} \frac{\rho_p \, r_i}{\rho} = 0 \tag{56}$$

Shear-Enhanced Coagulation[14]

$$K_{ij}^{Sh} = 4/3 \frac{\partial u}{\partial r} (r_i + r_j)^3$$

A code[2] (CRAM) implementing the model, but without turbulence or shear-enhanced terms already exists. It must be recoded to include these effects and to mate it to the nucleation model.

III. CONCLUSIONS

Documentation for a recent version of the LAPP code[1] has been developed to allow the extensive modification required for efficient performance. Equations for particle/gas interactions (dynamics) have been developed which

are suitable for inclusion into LAPP. A nucleation model[3] which fits naturally into the LAPP reaction kinetics format has been selected and the rate coefficients and thermochemical information necessary to implement it for the case of Si particle formation are being computed. A particle coagulation model[2] and a code implementing it are available. The effects of strong shear and turbulence on coagulation must be included and the code mated to LAPP.

IV. PLANS

During the next quarter the nucleation and coagulation models will be coded and inserted into LAPP. The particle/gas interaction equations will also be inserted. It is anticipated that the code containing these models will be run with a simple gas-phase kinetics model for the formation of Si (gas) in the $SiCl_4/Na/H_2/Ar$ chemical system. This model will include simple Cl abstraction reactions

$$SiCl_x + Na \rightarrow NaCl + SiCl_{x-1} \qquad (57)$$

as well as the usual reactions among species such as H, Cl, H_2, Cl_2, NaCl, and HCl. It will be assumed, as indicated by observation of $Na/SiCl_4$ flames, that processes represented by Reactions (57) are fast (gas kinetic) and thus the reaction will probably be mixing rate limited. (Since modeling the mixing, is, at best, an art, as indicated by the number of models for this process included in the code, there will be reliance on experiment to select the most reliable model. Any of the models will, however, give a semi-quantitative estimate of what can be expected for a mixing rate.)

Also during the next quarter, modeling efforts will be chiefly concerned with developing equations describing condensation onto and evaporation from particles in turbulent flows. The physical problem to be addressed here is that (i) for very small particles, evaporation and condensation will be rate limited not by the rate of diffusion to the particle surface, but by the surface chemistry process itself, (ii) for larger particles, diffusion may become rate limiting until (iii) the particles become too large to follow the gas-phase velocity fluctuations at which point surface rates may once again become important. Solving this problem, i.e., determining the particle sizes for

which changes in the rate limiting mechanism occur and writing the appropriate equations, will also bear directly on modeling of heterogeneous reactions (which will be treated later in the program).

V. NEW TECHNOLOGY

No reportable items of new technology have been identified.

VI. REFERENCES

1. Mikatarian, R.R., Kau, C.J., and Pergament, H.S., "A Fast Computer Program for Nonequilibrium Rocket Plume Predictions," Final Report, AeroChem TP-282, AFRPL-TR-72-94, NTIS AD 751 984, August 1972.

2. Hwang, B.C. and Gould, R.K., "Rocket Exhaust Ground Cloud/Atmospheric Interactions," Final Report, AeroChem TP-362, NASA CR-145255, 1977.

3. Bauer, S.H. and Frurip, D.J., "Homogeneous Nucleation in Metal Vapors. A Self-Consistent Kinetic Model," J. Phys. Chem. 81, 1015-1024 (1977).

4. Richtmyer, R.D. and Morton, K.W., Difference Methods for Initial-Value Problems (Interscience Publishers, New York, 1957).

5. JANAF Thermochemical Tables (Dow Chemical Company, Midland, MI, continuously updated).

6. Ferri, A.J., "Review of Problems in Application of Supersonic Combustion," J. Roy. Aeron. Soc. 68, 575-597 (1964).

7. Schlichting, H., Boundary Layer Theory (Pergamon Press, New York, 1955).

8. Ting, L. and Libby, P.A., "Remarks on the Eddy Viscosity in Compressible Mixing Flows," J. Aero. Sci. 27, 797-798 (1960).

9. Donaldson, C. duP. and Gray, K.E., "Theoretical and Experimental Investigation of the Compressible Free Mixing of Two Dissimilar Gases," AIAA J. 4, 2017-2025 (1966).

10. Sutherland, W., "The Viscosity of Gases and Molecular Force," London Edinburgh and Dublin Phil. Mag. and J. of Science--5th Series 36, 507-531 (1893).

11. Kritz. M.A., "Formation Mechanism of the Stratospheric Aerosol," Ph.D. Thesis, Yale University, 1975.

12. Fuchs, N.A., The Mechanics of Aerosols (Macmillan, New York, 1964).

13. Huang, C.M., Kerker, M., and Matijevic, E., "The Effect of Brownian Coagulation, Gradient Coagulation, Turbulent Coagulation, and Wall Losses upon the Particle Size Distribution of an Aerosol," J. Colloid Interfac. Sci. 33, 529-538 (1977).

14. Zebel, G., "Coagulation of Aerosols," Aerosol Science, C.N. Davies, Ed. (Academic Press, New York, 1966) Chap. 2.

TABLE I

NOMENCLATURE

$a_{1/2}$	defined by Eq. (23)
A	constant in expression for k_f (see Eq. (13))
$b_{1/2}$	defined under Eq. (15b)
B	activation energy (see Eq. (13))
c_p	specific heat of mixture $(\sum_i X_i c_{p_i})$
c_{p_i}	specific heat of ith species
D_i	diffusion (Brownian) coefficient for particles, ith mass class
f_{p_i}	ratio of actual drag coefficient to Stokes flow drag coefficient for particles, ith mass class
F_i	defined as $X_i/W(=Y_i/W_i)$ in units of, e.g., molecules of ith species per gram of fluid
F_{p_i}	number of particles per gram of fluid, ith mass class
g_i	Gibbs free energy of ith species at standard state (1 atm)
g_{p_i}	ratio of actual heat transfer coefficient to that for Stokes flow, ith mass class particles
ΔG	change in standard Gibbs free energy for a reaction, $\sum_i (g_i)$ products $- \sum_i (g_i)$ reactants
G_{ij}	particle velocity
h	enthalpy of mixture
h_i	enthalpy of ith species
h_{298_i}	heat of formation of ith species at T = 298 K
h_B	Boltzmann's constant
k_f	forward rate coefficient
k_r	backward rate coefficient
K	eddy viscosity coefficient
$\overline{K}$	eddy viscosity coefficient for Donaldson/Gray model (see Eq. (22))
K_{ij}	coagulation rate coefficient
Kn_i	Knudson number of particles, ith mass class
K_p	equilibrium constant
Le	Lewis number (laminar or turbulent)

m_i	mass of particles, ith mass class
$M_{1/2}$	Mach number at half radius, defined under Eq. (22)
N	temperature exponent in reaction rate equation (Eq. (13))
p	static pressure
Pr	Prandtl number (laminar or turbulent)
r	coordinate normal to jet centerline
r_i	particle radius, ith mass class
r_{in}	inner mixing zone radius
$r_{1/2}$	defined under Eq. (18b)
$\bar{r}_{1/2}$	defined under Eq. (17)
R	universal gas constant
Re	Reynolds number
T	static temperature
T_{p_i}	particle temperature for ith mass class
T_w	wall temperature
u	x component of velocity
u_{p_i}	x component of particle velocity, ith mass class
v	r component of velocity
$v_{g,i}$	particle sedimentation velocity, ith mass class
$\dot{w}_i$	rate of production of ith species
$\dot{w}_{p_i}$	rate of particle production, ith mass class
$\dot{w}^{(j)}$	rate of production from jth reaction
W	molecular weight of mixture $(\sum_i F_i)^{-1}$
W_i	molecular weight of ith species
x	coordinate parallel to jet centerline
X_i	mole fraction of ith species
Y_i	mass fraction of ith species

Greek

α	constant for external control of eddy viscosity (see Eqs. (15) to (21))
δ_i	particle mean free path, ith mass class

ε	eddy diffusivity for turbulent flow; defined as μ/ρ
η	defined by Eq. (15)
λ_g	molecular mean free path
μ	eddy viscosity for turbulent flow
μ_g	molecular viscosity
ν	kinematic viscosity
ρ	gas density
ρ_p	particle density
σ	emissivity
Ψ	stream function

Subscripts

e	evaluated at edge of mixing layer (free stream)
i	ith species
j	value at nozzle (jet) exit
p_i	particle mass class i
o	evaluated at axis of symmetry, r = 0

Miscellaneous

$\lvert \quad \rvert$	absolute value
$\left(\frac{\partial}{\partial\beta}\right)_\gamma$	partial derivative with respect to β; γ being held constant
$\sum_i$	summation over i species

☆U.S. GOVERNMENT PRINTING OFFICE: 1978-740-094/1410